Molecular Biology of the Cell
Vol. 16, 2566–2576, May 2005

Ionizing Radiation–dependent γ-H2AX Focus Formation Requires Ataxia Telangiectasia Mutated and Ataxia Telangiectasia Mutated and Rad3-related

Joanna D. Friesner,* Bo Liu,† Kevin Culligan,† and Anne B. Britt†

*Genetics Graduate Group and †Section of Plant Biology, University of California, Davis, Davis, CA 95616

Submitted October 14, 2004; Revised February 24, 2005; Accepted February 28, 2005
Monitoring Editor: Orna Cohen-Fix

The histone variant H2AX is rapidly phosphorylated at the sites of DNA double-strand breaks (DSBs). This phosphorylated H2AX (γ-H2AX) is involved in the retention of repair and signaling factor complexes at sites of DNA damage. The dependency of this phosphorylation on the various PI3K-related protein kinases (in mammals, ataxia telangiectasia mutated and Rad3-related [ATR], ataxia telangiectasia mutated [ATM], and DNA-PKCs) has been a subject of debate; it has been suggested that ATM is required for the induction of foci at DSBs, whereas ATR is involved in the recognition of stalled replication forks. In this study, using *Arabidopsis* as a model system, we investigated the ATR and ATM dependency of the formation of γ -H2AX foci in M-phase cells exposed to ionizing radiation (IR). We find that although the majority of these foci are ATM-dependent, ~10% of IR-induced γ-H2AX foci require, instead, functional ATR. This indicates that even in the absence of DNA replication, a distinct subset of IR-induced damage is recognized by ATR. In addition, we find that in plants, γ-H2AX foci are induced at only one-third the rate observed in yeasts and mammals. This result may partly account for the relatively high radioresistance of plants versus yeast and mammals.

INTRODUCTION

The induction of DNA double-strand breaks (DSBs) in eukaryotes triggers a number of protective responses including the upregulation of repair pathways, initiation of cell cycle arrest, and, in some organisms, the induction of programmed cell death. DSBs in actively dividing cells are particularly dangerous. Repair to form translocations and deletions can lead to loss of heterozygosity, which in turn leads to carcinogenesis in mammals or lethality in haploid yeast. For this reason all living things possess the ability to detect the presence of DSBs and relay this information to the cell cycle.

Two important protein kinases involved in sensing and signaling DNA damage in eukaryotes are *a*taxia *t*elangiectasia *m*utated (ATM) and *a*taxia *t*elangiectasia mutated and *r*ad3-related (ATR; Abraham, 2001; Sancar *et al.,* 2004). In mammals, ATM is critical for responses to DSBs and signals downstream cell cycle checkpoint regulators including *p53* and *Chk2* to coordinate apoptotic responses and/or cell cycle arrest (Fernandez-Capetillo *et al.,* 2002). In addition to checkpoint regulation, *ATM* responds to DSBs by interacting with proteins intimately involved in DNA repair such as the Mre11-Rad50-Nbs1 (M-R-N) complex (Gatei *et al.,* 2000; van den Bosch *et al.,* 2003) and RAD51 (Chen *et al.,* 1999). In comparison, ATR, in a complex with the ATR interacting protein (ATRIP), is thought to respond primarily to agents that block replication, recognizing stalled replication forks and then signaling to Chk1 and p53 to induce cell cycle arrest, replication restart, and apoptosis (Abraham, 2001). In striking contrast to *ATM*, *ATR* is an essential gene in mammals; defects in the murine homolog cause early embryonic lethality and loss of ATR in conditional knock-out embryonic stem cells rapidly induces death (Brown and Baltimore, 2000; de Klein *et al.,* 2000). This is thought to reflect a requirement for ATR in the normal replicative cycle (Brown and Baltimore, 2003; Dart *et al.,* 2004).

One of the earliest known responses to DSB induction is the phosphorylation of thousands of molecules of the histone variant H2AX at the break site (Rogakou *et al.,* 1998). Phosphorylated H2AX, known as γ-H2AX, forms "foci" at DSBs induced by ionizing radiation (IR; Rogakou *et al.,* 1999), meiosis (Mahadevaiah *et al.,* 2001), replication (Ward and Chen, 2001), and V(D)J recombination (Chen *et al.,* 2000). Recently, H2AX has been identified as one of the targets of mammalian *ATM* and *ATR* phosphorylation. Probably reflecting their somewhat specialized roles in DNA damage recognition and signaling, it was determined that γ-H2AX forms in an *ATM*-dependent manner in response to DSB-inducing agents such as X-rays, etoposide, and bleomycin, but not UV light or methyl methanesulfonate, agents that primarily induce DNA dimers and alkyl adducts, respectively (Burma *et al.,* 2001). In contrast, it was found that H2AX is phosphorylated in an *ATR*-dependent manner in situations where DNA synthesis is blocked. In response to hydroxyurea or UV light, *ATR*-mediated γ-H2AX foci were found in the majority of S-phase cells, whereas very few nonreplicating G1 cells had γ-H2AX foci after the same treatment (Ward and Chen, 2001). This, taken together with the facts that ATR-mediated foci colocalize with proliferating cell nuclear antigen (PCNA; Ward *et al.,* 2004) and that RPA-bound single-stranded DNA (ssDNA) is a good substrate for ATR/ATRIP binding (Zou and Elledge, 2003) suggests that the ATR/ATRIP complex binds ssDNA and phosphorylates H2AX at stalled replication forks.

This article was published online ahead of print in *MBC in Press* (http://www.molbiolcell.org/cgi/doi/10.1091/mbc.E04–10–0890) on March 16, 2005.

Address correspondence to: Anne B. Britt (abbritt@ucdavis.edu).

© 2005 by The American Society for Cell Biology

Recently, plants defective in homologues of both *ATM* and *ATR* were found to have a number of features in common with the mammalian mutants. Loss of *ATM* in *Arabidopsis thaliana* (*Arabidopsis*) causes meiotic defects, hypersensitivity to DSB-inducing agents, and an inability to properly induce IR-mediated transcription of several DNA repair genes (Garcia *et al.*, 2003). Similarly, defects in the mammalian homolog cause IR sensitivity, prevent activation of *ATM* interacting proteins (Shiloh, 2003), and affect meiosis (Barlow *et al.*, 1998). Additional hallmarks of mammalian *ATM* deficiency include severe growth defects and neurodegenerative disease (Shiloh, 2003). In contrast, plant *ATM* mutants do not exhibit obvious developmental defects in the absence of DNA damaging agents. *Arabidopsis ATR* knockout mutants are viable, fertile, and phenotypically normal in the absence of exogenous DNA damaging agents. Like human conditional *ATR* knockout lines, mutant *atr* plants are hypersensitive to replication antagonists, including UV light, aphidicolin, and hydroxyurea, and are defective in G2 checkpoints induced by these agents (Culligan *et al.*, 2004). Thus, many of *ATR's* and *ATM's* functions are conserved in plants and mammals.

In this article, using both immunoblotting and immunocytochemistry we demonstrate that *ATM* and *ATR*-dependent γ-H2AX induction is conserved in plants and that IR-dependent γ-H2AX foci are formed at less than one-third the rate of mammalian γ-H2AX foci, suggesting a lower rate of DSB induction in plants. Significantly, because we limit our examination to M-phase cells, we show that *ATR* contributes to IR-induced γ-H2AX focus formation in the absence of DNA replication, demonstrating a clear role for *ATR* in response to IR distinct from its role during S phase. Furthermore, using mutants defective in either or both of the *Arabidopsis ATM* and *ATR* homologues, we quantify the contributions of each to IR-induced γ-H2AX formation. These results suggest that ATM and ATR are recognizing two distinct classes of IR-induced DNA damage products.

MATERIALS AND METHODS

Plant Lines and Human Cells

Wild-type, *atr-3*, and *atm-1* plants are in the *Ws* ecotype, and *atm-2* is in the *Col* ecotype (Garcia *et al.*, 2003; Culligan *et al.*, 2004). *atm,atr* double mutant plants were constructed using the *atm-1* and *atr-3* alleles. The *atm,atr* double mutant is completely sterile; to isolate double mutants, we PCR-genotyped progeny of an *atr-3* homozygous *atm-1* heterozygous plant, which is fertile and produces seeds that segregate in the expected 1:2:1 manner for *atm* in a homozygous *atr* background. Plants for protein extraction were grown on Premier Prosoil mix (Premier Horticulture, Dorval, Canada), whereas plants for root tip excision were grown on nutritive MS agar; all plants were grown at 21°C as described (Friesner and Britt, 2003). Human HCT116 colorectal cells, graciously donated by Dr. Ken Kaplan (UC Davis), were grown and maintained as described (Green and Kaplan, 2003).

Ionizing Radiation

Plants for protein extraction were sown on soil as described (Friesner and Britt, 2003). Approximately 3-wk-old single mutant plants (before bolting), or 4–6-wk-old double mutant plants with buds removed, were irradiated at doses indicated in the figures, with a ^{137}Cs source (7.5 Gy min^{-1}; Institute of Toxicology and Environmental Health, University of California, Davis). Plants were harvested at times indicated, placed into liquid nitrogen, and then stored at −80°C until protein extraction. Seeds grown for root tip excision were sterilized and plated onto nutritive agar as described (Friesner and Britt, 2003). Five- to 8-d-old seedlings were irradiated at doses indicated and immersed in fixative at times indicated, and root tips were excised (see *Root Tip Excision*, below). Plants involved in repair time course studies were returned to growth chambers and harvested at times indicated. Flasks of HCT116 cells were exposed to 100 Gy of IR or mock-irradiated, trypsin-harvested 30 min later, lysed, and subject to acid extraction as described (Karlsson and Stenerlow, 2004). After removal from incubation, cells were kept at room temperature before extraction.

Antibody Production

Anti- plant γ-H2AX antibody was prepared by AnaSpec (San Jose, CA) against the synthetic peptide CVGKNKGDIGSA(p)SQGEF (the cysteine was added during preparation). These amino acids are identical in both the putative *Arabidopsis* H2AX proteins H2AXa and H2AXb. The peptide was conjugated to keyhole limpet hemocyanin and injected into two rabbits. Immune serum was first passed over a column containing immobilized CVGKNKGDIGSA(p)SQGEF to retain phospho-specific antibodies, eluted, and passed over a second column containing immobilized CVGKNKGDIGSASQGEF to remove antibodies to unphosphorylated H2AX. The flow-through from this column was used in experiments in this study. ELISA analysis was performed by AnaSpec to demonstrate the specificity of the antibody to phosphorylated H2AX peptide.

Acid Extraction of Proteins

To enrich samples for histones, acid extraction of plant tissue was performed essentially as described (Jackson *et al.*, 2004), with the following modifications; Sodium fluoride (Acros, Morris Plains, NJ) and sodium ortho-vanadate (Acros) were added to concentrations of 30 and 100 mM, respectively, to inhibit protein phosphatases. Protein samples were quantified using the Bio-Rad Protein Assay (Bio-Rad Laboratories, Richmond, CA), using bovine serum albumin (BSA) to create a standard curve. Human HCT116 cells were acid extracted as described (Karlsson and Stenerlow, 2004) with benzamide and aprotinin omitted. Protein concentration was estimated by comparing serial dilutions of samples on a gel stained with Coomassie-blue. Five percent 2-mercaptoethanol, 5–10% 1.5 M Tris-HCl, pH 8.8 (to neutralize samples, if needed), and 5× sample loading buffer (10% SDS, 0.5% bromophenol blue, 313 mM Tris-HCl, pH 6.8, 50% glycerol) were then added to each tube, and samples were boiled for 5 min. Samples were stored at −20°C until used for immunoblotting. Before loading, samples were reboiled for 3 min.

Immunoblotting

For plant protein blots, ~20 μg of protein samples was loaded into each well of a 4–20% Tris-glycine-SDS gradient precast polyacrylamide gel (iGel, Gradipore, Hawthorne, NY) before electrophoresis. Gels were transferred to PVDF membranes (Immobilon-P, Millipore, Bedford, MA) overnight at 95 mA, 4°C with either CAPS/methanol buffer (10 mM CAPS, 10% methanol, pH 11) or nonmethanol buffer (48 mM Tris base, 39 mM glycine, to pH 9.3 with NaOH). Blots were incubated in 3% skim milk in 1× Tris-buffered saline (TBS)-T (0.05% final concentration Tween-20) either overnight at 4°C, or at room temperature for 3–5 h, on a rotating platform. Blots were then incubated overnight at 4°C in rabbit antiplant γ-H2AX primary antibody diluted 1:5000 in 3% skim-milk/1× TBS-T. Blots were briefly rinsed three times with ddH_20, washed three times for 5 min each in large volumes of ddH_20, and then once in 1× TBS-T for 15 min at room temperature on a rotating platform. Blots were then incubated with anti-rabbit immunoglobulin horseradish peroxidase–linked secondary antibody (Amersham Biosciences NA934V, Piscataway, NJ) at a dilution of 1:10,000 in 3% skim milk/1× TBS-T for 1–2 h at room temperature on a rotating platform. Blots were washed as before and exposed for various times, typically 45 s to 5 min, to x-ray film (Hyperfilm ECL, Amersham Biosciences; or CL-Xposure film, Pierce, Rockford, IL) after incubation with enhanced chemiluminescence reagents (ECL+) as described (RPN 2132, Amersham Biosciences). After film exposures, blots were stained for 5 min in Ponceau S (P-3504, Sigma, St. Louis, MO) solution, and destained with ddH_20 to visualize proteins and estimate protein loading. For Western blots containing human cell, protein samples were separated on a 12.5% polyacrylamide gel and transferred to nitrocellulose membranes for 4 h at 400 mA and 4°C using 20% methanol transfer buffer. Blots were incubated in 2% nonfat dry milk in 1× TBS-T for 1 h at room temperature. Blots were incubated for 2 h at room temperature in either polyclonal anti-human γ-H2AX primary antibody (Upstate Biotechnology, Lake Placid, NY) diluted 1:1000 or polyclonal antiplant γ-H2AX primary antibody diluted 1:4000 in phosphate-buffered saline (PBS)-gelatin. Blots were washed and incubated for 1 h at room temperature in anti-rabbit secondary antibody as described above. Blots were exposed to x-ray film as described above, except the SuperSignal West Pico detection system by Pierce was used as directed. Film exposures and Ponceau S–stained blots were scanned to retain digital images.

Root Tip Excision and Slide Preparation

Root tips were excised as described (Liu *et al.*, 1993), with the following modifications: root tips were fixed for 45 min in freshly prepared 4% formaldehyde solution in 1× PME and then washed with 1× PME five times for 5 min each. Tips were digested for 30 min in a 1% cellulase solution (Onuzuka RS cellulase, Research Products International, Mount Prospect, IL) prepared in 1× PME and washed five times for 5 min with 1× PME as before. Root tips were squashed gently onto gelatin-coated slides as described (Liu *et al.*, 1993); slides were allowed to air dry and placed at −80°C until antibody incubation. Before immunostaining, slides were removed from −80°C, warmed at room temperature for 15–25 min, and rehydrated in 1× PME. Slides were incubated with 0.5% Triton X-100 (Sigma) in 1× PME for 10–15 min, rinsed with 1× PME, incubated three times for 5 min in 1× PME, and then immersed in

−20°C methanol for 10 min. Slides were immediately placed in 1× PBS for 10 min and then washed three times for 5 min with 1× PBS. All washes were performed at room temperature.

Immunostaining

Slides were incubated with our rabbit antiplant γ-H2AX and commercially available mouse monoclonal antialpha tubulin (Sigma, clone DM1A) antibodies. Antibodies were diluted 1:400–1:800 for anti-γ-H2AX, and 1:600–1:800 for anti-α-tubulin in dilution solution (3% BSA, 0.05% Tween-20, 0.02% NaN_3 in 1× PBS, stored at 4°C). Fifty microliters of diluted primary antibodies were applied to each slide for 3 h at room temperature or overnight at 4°C. Slides were washed three times in 1× PBS for 5 min each and incubated for 2–3 h at room temperature in 50 μl antibody dilution solution consisting of FITC-conjugated donkey anti-rabbit (Rockland Immunochemicals, Gilbertsville, PA, 1:800 or 1:1000) or Alexa 488–conjugated goat anti-rabbit (Molecular Probes, Eugene, OR, 1:800 or 1:1000) and Texas red-X–conjugated goat anti-mouse (Molecular Probes, 1:800 or 1:1000) secondary antibodies. Slides were washed as before. Finally, slides were mounted in DAPI-containing mounting medium to visualize plant chromosomes (100 mM Tris-HCl, pH 9.2, 50% glycerol, 2 μg/ml DAPI, 1 μg/ml phenylene diamine, stored at −80°C); coverslips were applied and sealed with clear nail polish, and slides were placed at 4°C overnight before examining. Nuclei were visualized using a Nikon Eclipse E600 epi-fluorescence microscope (Melville, NY) equipped with a mercury lamp. Images were viewed using ImagePro Plus software (Media Cybernetics, Silver Spring, MD) and captured using a Hamamatsu digital camera (C4742–95, Bridgewater, NJ), equipped with a UniBlitz shutter driver (model D122). Images were captured using a 100× oil lens, and exported as 24-bit RGB composite images, and 8-bit grayscale individual images. A scale bar was drawn in Adobe Photoshop (San Jose, CA) after capturing an image of a micrometer (AO, 0.1 mm/10 μm divisions) at 100× magnification. A 5-μm scale bar was inserted into unmanipulated images and then resized as part of the image.

RESULTS

Putative Arabidopsis H2AX Protein Homologues

The presence of H2AX sequence homologues in widely divergent organisms including *Homo sapiens*, *Saccharomyces cerevisiae,* and *Arabidopsis* (Redon *et al.,* 2002) suggests that these proteins are conserved throughout eukaryotes. Our search of the *Arabidopsis* genome database, using the human H2AX amino acid sequence as a query, revealed two putative H2AX protein homologues that we term *H2AXa* and *H2AXb*. The genes encoding the proteins are located ~17 Mb apart on opposite sides of the centromere on Chromosome I. Both predicted proteins are 143 amino acids in length and differ in only two positions: *H2AXa* (GenBank locus At1g08880) codes for threonine at position 3, whereas *H2AXb* (GenBank locus At1g54690) codes for serine, and at position 44, *H2AXa* codes for serine, whereas *H2AXb* codes for alanine. Both possess the canonical C-terminal SQ motif shared by all H2AX protein homologues that is the site of DNA DSB-induced phosphorylation. Histones are highly conserved proteins in eukaryotes, and 13 putative *Arabidopsis* H2A homologues have been identified in the plant chromatin database (http://www.chromdb.org/). Of these sequences, H2AXa and H2AXb share more identity throughout their coding regions than either shares with any other H2A homolog, suggesting that they may represent a recent gene duplication event (Arabidopsis Genome, 2000; Mitchell-Olds and Clauss, 2002). Expressed sequence tags (ESTs) for both genes are present in GenBank, indicating that both are transcribed, but functional data will be needed to demonstrate whether the two genes have distinct or overlapping roles.

In addition to these two putative H2AX homologues, we found a third *Arabidopsis* mRNA sequence in GenBank (locus tag BT002503) more closely related to the human H2AX sequence than the previous two. The amino acid sequence corresponding to the translated mRNA was so similar to the human sequence that when used in a database search, the most significant matches were mammalian, rather than plant sequences. Furthermore, BLAST searches could not map the mRNA sequence to any *Arabidopsis* chromosomal locus, suggesting it was encoded by a different organism. The sequence is probably an incorrectly labeled database contaminant, presumably of mammalian origin.

A Plant-specific γ-H2AX Antibody Recognizes an IR-induced Antigen in Plant and Human Cells

Previous research had demonstrated that an antibody raised against the C-terminus of human γ-H2AX could detect H2AX phosphorylation in *Xenopus laevis*, *Drosophila melanogaster*, and *S. cerevisiae,* suggesting it might similarly cross-react with plant γ-H2AX (Rogakou *et al.,* 1999). We obtained both monoclonal and polyclonal antibodies raised against the C-terminus of human γ-H2AX (Upstate Biotechnology) and performed immunoblotting of irradiated and unirradiated plants. We found that the human antibodies detected a faint 16-kDa protein in plant extracts, approximately the predicted size for plant γ-H2AX, but the level of cross-reactivity was low and in some blots the protein was observed in both irradiated and unirradiated samples (unpublished data). This lack of specificity for irradiated plant tissues suggested that either plant H2AX is always phosphorylated to some extent, or that, regardless of the high degree of similarity between the plant and human proteins, some critical difference must allow the antibody to also recognize unphosphorylated plant H2AX and/or some other protein of similar size.

Because of the low cross-reactivity of the human γ-H2AX antibody for irradiated plant extracts, we generated an antibody to the putative plant homologues. A synthetic peptide corresponding to the phosphorylated C-terminal 14 amino acids of *Arabidopsis* γ-H2AX (identical in *H2AXa* and *H2AXb*) was synthesized and a polyclonal antibody was raised in rabbits. The plant γ-H2AX antibody recognized an ~16-kDa protein in extracts made from irradiated wild-type plants. The antibody also recognized a minimal background band that comigrated with γ-H2AX in unirradiated plants; this may represent a very low steady state level of phosphorylated H2AX, recognition of the nonphosphorylated protein by the polyclonal antibodies, or recognition of some unrelated protein. Within 2 min after treatment with 50 Gy, a dose requiring approximately 7 min of IR exposure, we observed a strong induction of γ-H2AX (unpublished data) that reached maximal amounts within 20 min (Figure 1A). Our plant γ-H2AX antibody detected an IR-induced 16-kDa protein in human cells as well, although detection of this signal required a larger application of protein to the blot (Figure 2). In contrast, a commercially available human antibody, although recognizing both the plant and animal IR-induced protein, was able to detect the human protein with much greater sensitivity (unpublished data). The fact that both the human and plant antibodies detect the same IR-induced signal in both plant and animal cells indicates that our antibody is indeed detecting γ-H2AX. The identity of the higher molecular weight protein at ~28 kDa is not known (Figure 1) but it typically appears in all samples, regardless of IR exposure. We believe these bands may represent background cross-reacting protein; however, we do observe some variability in the presence and prominence of this high-molecular-weight protein between immunoblots.

Induction of Plant γ-H2AX Is IR Dose Dependent

Protein samples from wild-type *Arabidopsis* plants exposed to increasing doses of IR were subjected to immunoblotting and probed with the plant γ-H2AX antibody. We observed a

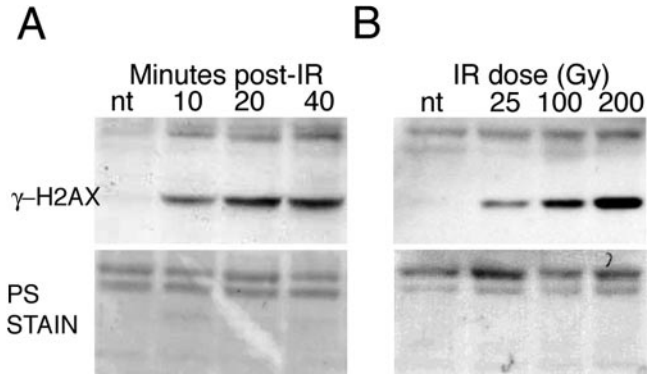

Figure 1. γ-H2AX protein induction in wild-type plants. (A) γ-H2AX induction was assessed over a time course of 10–40 min by immunoblotting. Plants were irradiated with 50 Gy of IR and harvested at the times indicated, which included the time required to deliver the radiation (~7 min). (B) γ-H2AX induction assessed after increasing doses of IR. Plants were treated with IR as indicated and harvested 15 min after removal from the gamma source. Immunoblots were stained with Ponceau S (PS) and the major protein bands at the top of the blot were compared with qualitatively control for protein loading. Figures are representative blots from two experiments. nt, not treated with IR.

strong induction of γ-H2AX after IR exposure and protein levels increased with dose (Figure 1B). These data support the prediction that by increasing IR dose, H2AX protein phosphorylation will increase in response to higher levels of DNA damage and suggests that plant γ-H2AX may serve as an indicator of DSB induction in the plant genome.

IR-induced γ-H2AX Foci in M-phase Nuclei

Even correcting for its small genome size, *Arabidopsis* is a relatively radiation-resistant organism. For this reason we are interested in determining whether the rate of DSB formation by IR is reduced in plants. In mammalian cells, the appearance of γ-H2AX foci clearly correlates with DSB induction, and its loss, with DSB repair (DSBR) (Rothkamm and Löbrich, 2003). Given the obvious value of this assay for DSB induction and repair, identifying an analogous plant process would contribute significantly to our ability to elucidate similar and/or unique features of plant DSBR.

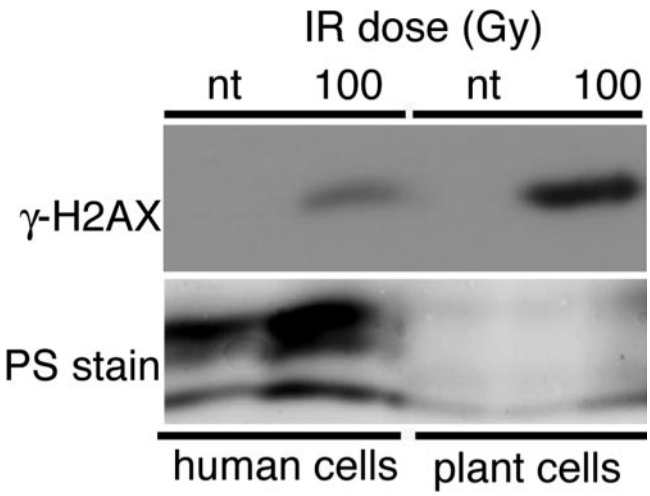

Figure 2. Protein recognition by the antiplant γ-H2AX antibody in irradiated human cells. Human HCT116 colorectal cells were exposed to 100 Gy of IR and harvested 30 min after removal from the gamma source. A membrane containing equal amounts of irradiated and mock-irradiated protein samples was probed with the plant γ-H2AX antibody. Plant samples were included in the experiment for comparison. PS stain, Ponceau S stain as in Figure 1. nt, not treated with IR.

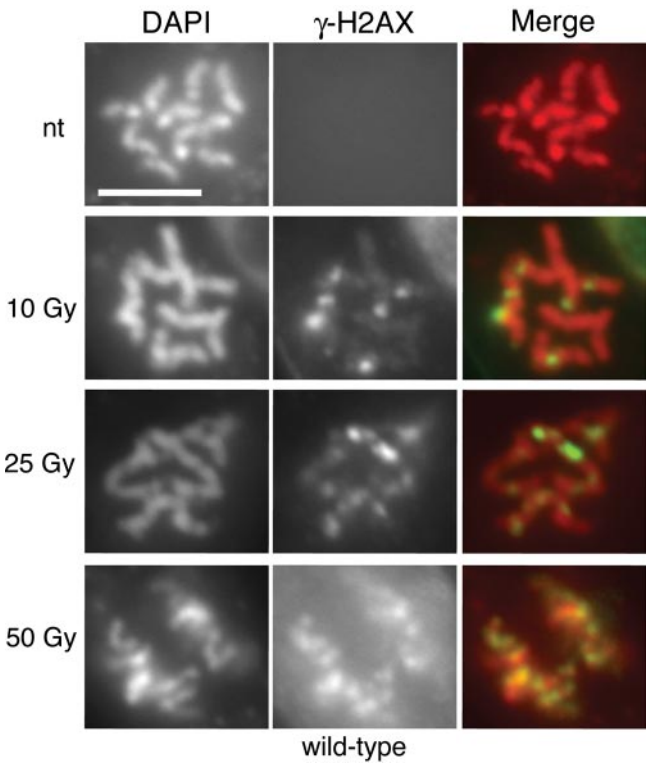

Figure 3. γ-H2AX focus formation in wild-type plants. Immunofluorescence of root tip nuclei demonstrates IR-dependent γ-H2AX focus induction. Wild-type plants were irradiated with increasing doses of IR and then paraformaldehyde-fixed 5 min after removal from the gamma source. DNA is visualized with DAPI, and merged images overlay γ-H2AX foci onto chromosomes. Scale bar, 5 μm. nt, not treated with IR.

To determine whether plant γ-H2AX foci could also be visualized in response to IR-induced damage, we performed in situ immunostaining experiments using *Arabidopsis* root tip nuclei. However, most of the DNA in plant cells is endoreduplicated to varying degrees, confounding our ability to accurately determine the number of foci per Gy per Gbp (gigabase pair). Thus, we chose to look at M-phase cells, which in the primary root tip meristem are strictly diploid (D'Amato, 1964). We did not observe any γ-H2AX foci in unirradiated wild-type M-phase cells, but discrete, chromosomally located γ-H2AX foci appeared very quickly after exposure to IR. The intense, localized γ-H2AX staining on chromosomes made it possible to count individual foci (Figure 3). Induction of foci by gamma was approximately linear with dose (Table 1, Figure 4). If we assume the diploid replicated (4N) *Arabidopsis* genome of an M-phase cell is ~500 Mbp, this corresponds to ~1.1–2 foci/Gy-Gbp.

γ-H2AX Induction and Disappearance in Repair-proficient Plants

It has been demonstrated that each γ-H2AX focus is equivalent to one DSB (Rogakou *et al.*, 1999), and disappearance of

Table 1. γ-H2AX focus formation in wild-type plants

	Dose				
	0 Gy	2.5 Gy	5 Gy	10 Gy	25 Gy
Average no. of foci/cell					
Trial 1	0 ± 0 (6)	2.75 ± 0.28 (16)	3.91 ± 0.23 (28)	6.4 ± 0.24 (24)	14.3 ± 1.14 (6)
Trial 2	0 ± 0 (13)	2.38 ± 0.12 (45)	4.53 ± 0.33 (18)	6.2 ± 0.22 (20)	12.7 ± 1.20 (3)
Overall	0 ± 0 (19)	2.48 ± 0.12 (61)	4.16 ± 0.19 (46)	6.3 ± 0.16 (44)	14.1 ± 0.89 (9)

Values are ± SE with the number of cells in parentheses.

γ-H2AX is a reliable indicator of DSBR in mammalian cells (Rothkamm and Löbrich, 2003). To determine the rate at which plant γ-H2AX disappears after induction, we irradiated wild-type plants and harvested tissue after allowing variable time for DNA repair. Similar to our previous experiments, immunoblotting revealed a large initial induction of γ-H2AX in plants harvested shortly after irradiation (Figure 5). Within 2 h, the majority of γ-H2AX had disappeared, and by 48 h postirradiation, γ-H2AX staining had decreased to unirradiated levels, suggesting that most DSBs are repaired quite rapidly in wild-type plants, and only a small number of IR-induced lesions persist. The different rates of γ-H2AX loss we observe may represent the well-characterized phenomenon of differential rates of DSBR (Glasunov *et al.*, 1989; Kodym and Horth, 1995; Iliakis *et al.*, 2004); although the majority of DSBs are quickly repaired, a small subset, perhaps requiring more time and/or different repair complexes for resolution, persist (Nazarov *et al.*, 2003). An alternative, but not exclusive possibility, is that some of the persisting fraction represents indirectly induced DSBs triggered by replication fork collapse in S-phase cells, or γ-H2AX focus formation at non-DSB lesions (Limoli *et al.*, 2002; Ward *et al.*, 2004).

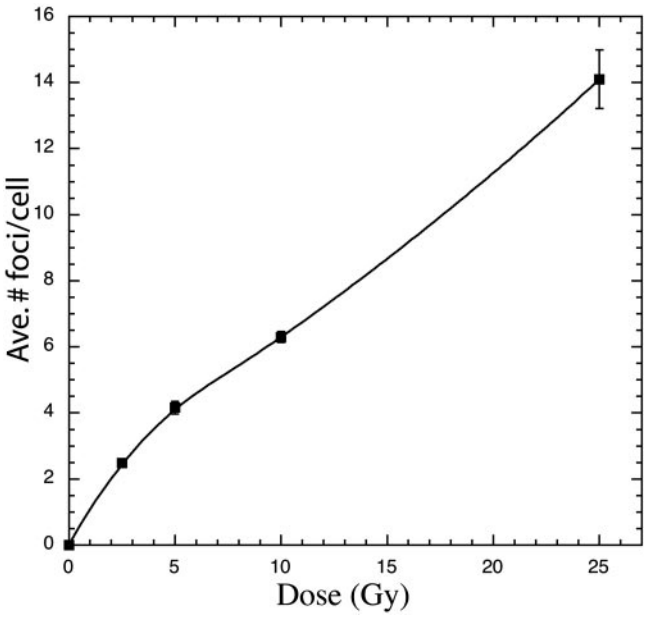

Figure 4. Approximately linear induction of γ-H2AX foci as a function of IR dose. Error bars, SEM of the values obtained from two experiments. Except for the 25-Gy data point, SEM bars are smaller than the data point symbols.

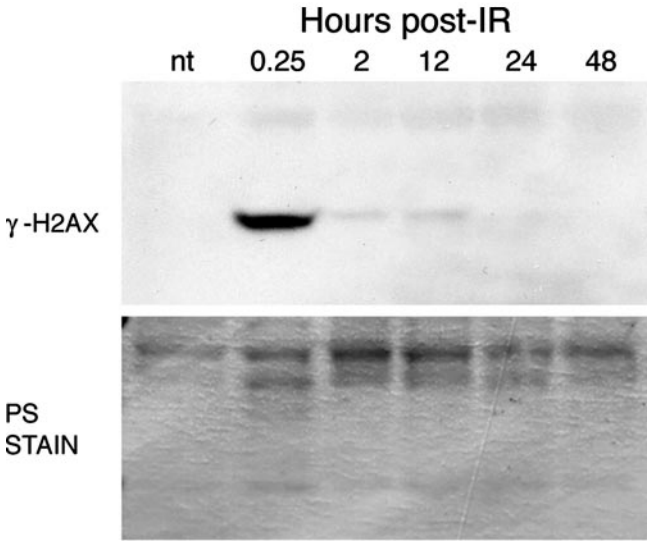

Figure 5. γ-H2AX induction and disappearance in wild-type plants. Plants received 100 Gy of IR and then were returned to growth chambers and harvested at the times indicated. The immunoblot is representative of four experiments. PS stain, Ponceau S stain as in Figure 1. nt, not treated with IR.

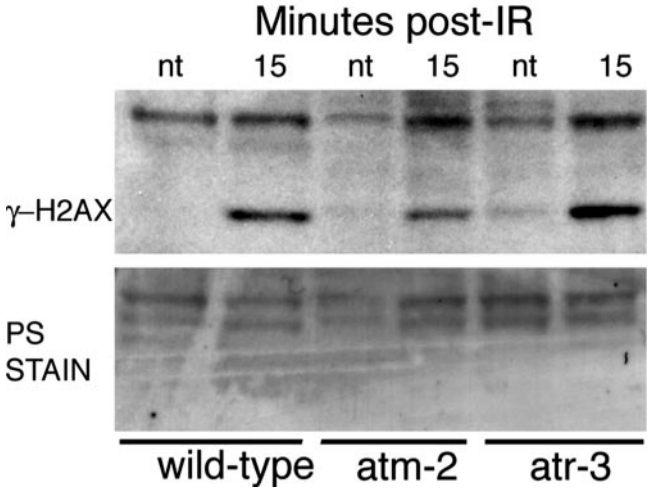

Figure 6. γ-H2AX induction in *atm* and *atr* mutants. Immunoblot of wild-type, *atm*, and *atr* plants, in the presence or absence of IR. Plants were irradiated with 100 Gy and harvested 15 min after removal from the gamma source. PS, Ponceau S stain as in Figure 1.

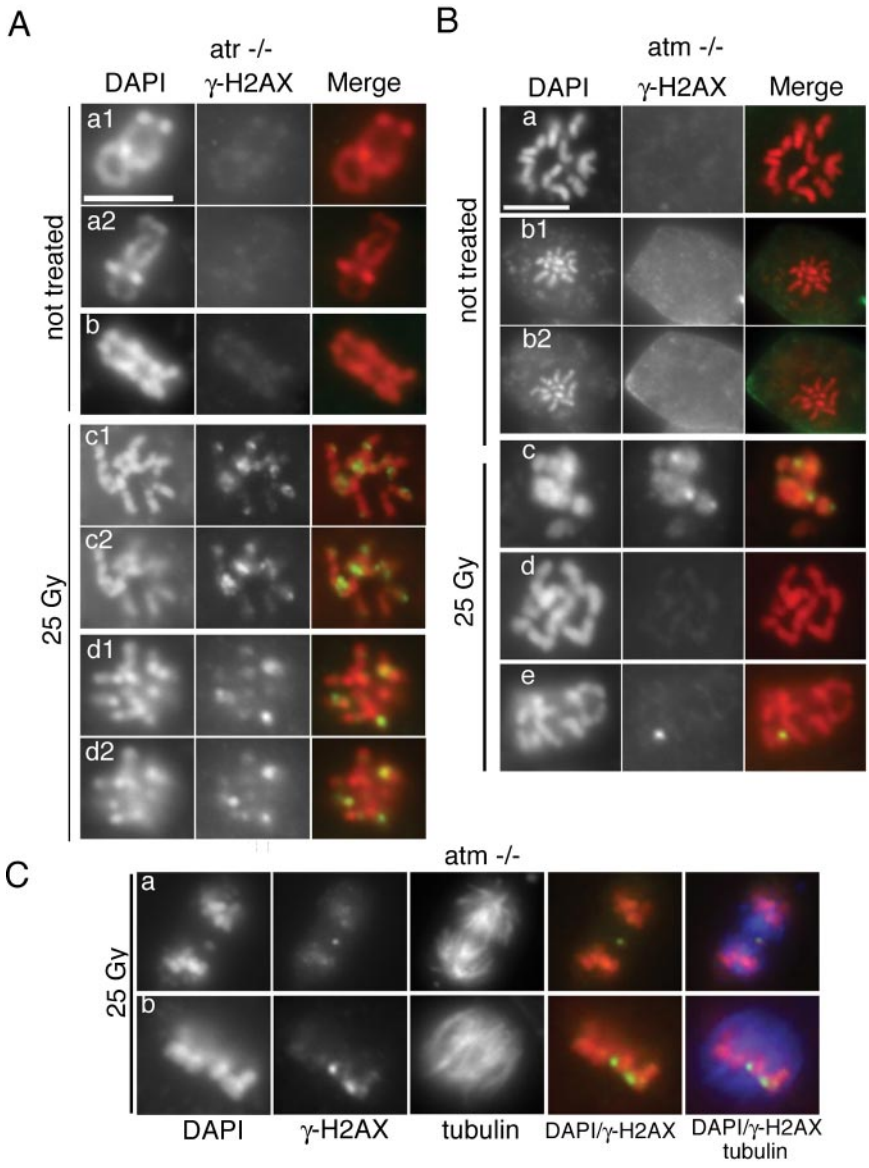

Figure 7. γ-H2AX induction in *atm* and *atr* mutants. (A) IR-dependent γ-H2AX focus formation detected by immunofluorescence in *atr* mutant plants. (a1 and a2) Two focal planes of one unirradiated cell; (b) one focal plane of another unirradiated cell. (c1 and c2) Two focal planes of one cell; (d1 and d2) two focal planes of a different cell treated with 25 Gy. (B) IR-dependent γ-H2AX focus formation detected by immunofluorescence in *atm* mutant plants. (a and b1/b2) Two unirradiated *atm* nuclei, the second with two focal planes shown. (c–e) A single focal plane from three *atm* nuclei exposed to 25 Gy. Scale bar, 5 μm. (C) γ-H2AX foci in *ATM*-deficient cells going through anaphase (a) or late metaphase (b). Mitotic microtubules are marked with mouse anti-α-tubulin antibodies and visualized in conjunction with γ-H2AX foci and plant chromosomes. nt, not treated with IR.

AtATR and AtATM Have Complementary Roles in IR-induced γ-H2AX Formation

To determine if either *AtATM* or *AtATR* are responsible for the phosphorylation of histone H2AX in response to ionizing radiation, we examined γ-H2AX induction in *atm* and *atr* mutant plants. In this study, we used two alleles of *ATM*, *atm-1* and *atm-2* (Garcia *et al.,* 2003), and one of *ATR*, *atr-3* (Culligan *et al.,* 2004). All three lines were generated by T-DNA insertional mutagenesis and each contains a T-DNA insertion in the 3′ region of the gene. The mutation in *atm-1* prevents *ATM* protein expression, and *atm-2* is phenotypically indistinguishable from *atm-1*, suggesting both are null alleles. Both are sensitive to IR and defective in meiosis (Garcia *et al.,* 2003). The insertion in *atr-3* lies in the highly conserved C-terminal kinase domain and RT-PCR analysis confirms the *ATR* transcript is absent, suggesting it is also a null allele (Culligan *et al.,* 2004).

We observed IR-dependent γ-H2AX induction in wild-type, as well as *ATM*- and *ATR*-deficient plants via immunoblotting (Figure 6). To support these qualitative data we quantified IR-induced γ-H2AX foci in *atm* and *atr* root tips. While γ-H2AX foci were readily apparent in *atr* nuclei (Figure 7A), the number was severely reduced in *atm* nuclei (Figure 7B). Typically, one or two foci were seen in *atm* nuclei, and ~25% had no foci at all. In comparison to wild-type plants, which have ~14 foci per cell at this dose (25 Gy), the average number of γ-H2AX foci was 10.5 ± 0.31 in *atr* plants and 1.2 ± 0.17 in *atm* plants (Table 2). Because the foci averages for wild-type and *atr* plants were close in value, and because at this dose, some foci overlap, we also examined *atr* plants after 10 Gy of IR. Similar to the data at 25 Gy, foci induction in *atr* plants was slightly, but significantly, reduced after 10 Gy in comparison to wild-type plants (Figure 8). The level of focus formation in *atm* plants was somewhat puzzling given the immunoblot data that suggested loss of *AtATM* caused only a slight reduction in γ-H2AX induction in comparison to wild-type plants (Figure 6). It may be that the differences we observe in the two methods of examining γ-H2AX induction are due merely to the qualitative nature of our immunoblots. Alternatively, it is possible that the fairly robust γ-H2AX induction observed in *atm* mutants in Figure 6 is due to the use of cycling cells in

Table 2. *AtATR* and *AtATM* both contribute to γ-H2AX focus formation

	Dose		
Plant line	0 Gy	10 Gy	25 Gy
Wild-type			
Trial 1	0 ± 0 (6)	6.4 ± 0.24 (24)	14.8 ± 1.14 (6)
Trial 2	0 ± 0 (13)	6.2 ± 0.22 (20)	12.7 ± 1.20 (3)
Overall	0 ± 0 (19)	6.3 ± 0.16 (44)	14.1 ± 0.89 (9)
atr			
Trial 1	0 ± 0 (14)	5.3 ± 0.29 (17)	10.3 ± 0.80 (6)
Trial 2	0 ± 0 (14)	5.5 ± 0.29 (23)	10.5 ± 0.31 (14)
Overall	0 ± 0 (28)	5.4 ± 0.21 (30)	10.5 ± 0.89 (20)
atm			
Trial 1	0 ± 0 (24)		1.4 ± 0.26 (12)
Trial 2	0 ± 0 (23)		1.1 ± 0.22 (19)
Overall	0 ± 0 (47)	n.d.	1.2 ± 0.17 (31)
atm,atr			
Trial 1			0 ± 0 (3)
Trial 2			0 ± 0 (5)
Trial 3			0 ± 0 (7)
Overall	n.d.	n.d.	0 ± 0 (15)

Values are the average number of foci/cell ± SE, with the number of cells in parentheses. Data are from Table 1. n.d., not determined.

immunoblotting experiments while we limit our examination to M-phase cells during immunofluorescent microscopy. Some proportion of cycling cells will be undergoing replication at the time of IR exposure and it is well established in mammalian cells that γ-H2AX induction is primarily dependent on *ATR*, rather then *ATM*, during S phase (Ward and Chen, 2001). It is possible that some of the γ-H2AX observed in *atm* immunoblots is due to ATR-dependent H2AX phosphorylation at sites of IR-induced replicational stress.

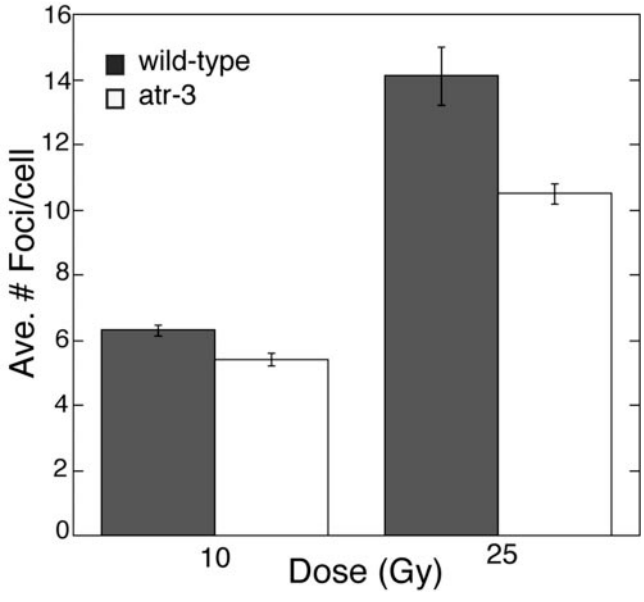

Figure 8. γ-H2AX induction in wild-type and *atr* plants. Comparison of γ-H2AX focus induction averages from wild-type and *atr* plants exposed to 10 or 25 Gy. Error bars, SEM of the values obtained from two experiments.

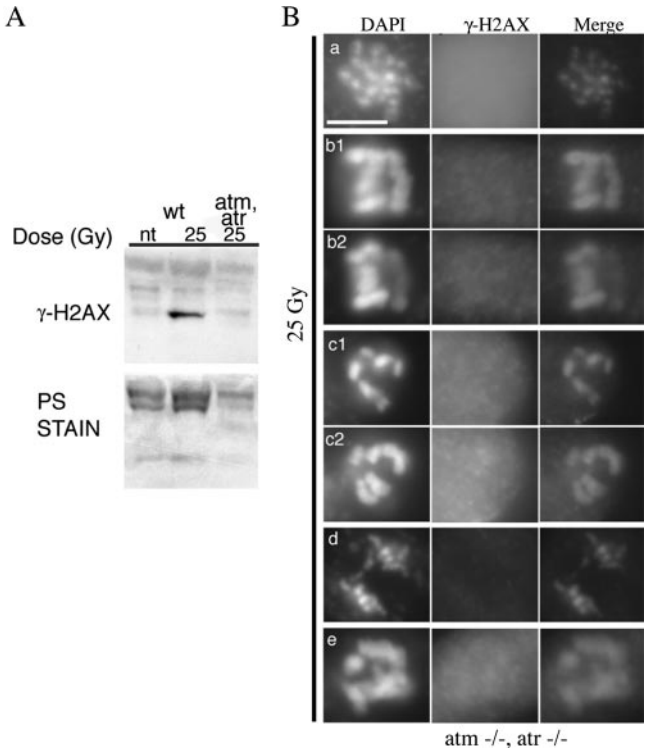

Figure 9. γ-H2AX induction in *atm,atr* double mutant plants. (A) Immunoblot of wild-type and *atm,atr* plants. Plants were treated with 25 Gy and harvested 15 min after removal from the gamma source. The immunoblot is representative of three experiments. PS stain as in Figure 1. (B) IR-dependent γ-H2AX focus formation detected by immunofluorescence in *atm,atr* double mutant plants. (a) One focal plane of a single nucleus; (b1/b2 and c1/c2) two focal planes each of two separate nuclei; (d and e) one focal plane of two separate nuclei. All nuclei are from plants irradiated with 25 Gy. Scale bar, 5 μm. n.t., not treated with IR.

These data suggest that both *AtATR* and *AtATM* are involved in the IR-induced phosphorylation of H2AX and that *AtATM* is directly or indirectly responsible for the majority (~90%) of focus formation in M-phase cells. The low residual number of foci in *atm* plants suggests that, in the absence of *ATM*, another kinase can phosphorylate H2AX in response to IR; one obvious candidate is *ATR*. To determine if the ATR homolog was responsible for the few remaining IR-induced foci in *atm* plants, we examined γ-H2AX induction in an *atm,atr* double mutant. In contrast to wild-type, *atm*, and *atr* single mutant plants (Figure 6), no γ-H2AX induction was observed in immunoblots of *atm,atr* double mutants after IR exposure (Figure 9A). To confirm these data, *atm,atr* seedlings were irradiated with 25 Gy, and root tip nuclei examined for the presence of γ-H2AX foci. As expected based on the immunoblotting data, no γ-H2AX foci were observed in *atm,atr* nuclei (Figure 9B, Table 2). These data suggest that although formation of most γ-H2AX foci is dependent on *AtATM, AtATR* is capable of phosphorylating a limited subset of IR-induced lesions.

It is known that *ATR*-dependent γ-H2AX foci form in response to replicational stress (Ward *et al.*, 2004) raising the obvious question of whether the foci observed in *atm* plants were from cells exposed to IR while in S phase. Plants were harvested between 5 and 20 min after irradiation and all cells examined were in prometaphase or later, well past nuclear envelope breakdown, a process requiring more than

Table 3. Lower DSB induction in plants

Organism	Average no. of foci or DSBs per Gy-Gbp	Reference
Arabidopsis	1.25–2[a]	This study
Tobacco		
BY-2 cells	2.0[b]	Yokota *et al.* (2005)
Yeast (*S. cerevisiae*)	5.4[b]	Prise *et al.* (1998)
CHO-K1 cells	6.6,[b] 5.5[b]	Yokota *et al.* (2005),[b] Cedervall *et al.* (1995)[b]
Human fibroblasts	6.0,[a] 6.5[b]	Rothkamm and Lobrich (2003)

[a]Foci or [b]DSBs.

20 min to complete (Wolniak and Larsen, 1992; Hush *et al.*, 1996; Vos *et al.*, 2000). Thus, it is clear that the *ATR*-dependent foci seen in *atm* mutants are induced during mitosis rather than in the preceding S phase. We used an antibody against tubulin to visualize the mitotic spindle and determine the phase of all cells examined; in one experiment, 24 of 32 *atm* cells were in anaphase or metaphase with the remainder in prometaphase (Figure 7C). In the absence of both *AtATM* and *AtATR*, γ-H2AX induction in response to IR is completely abrogated, suggesting both play a role in response to IR-induced DNA damage. Given that the average number of foci is reduced in each mutant, these data might be further interpreted to suggest that each kinase recognizes a discrete subset of IR induced lesions in M-phase cells.

DISCUSSION

Data suggest that plants are more resistant than mammals to the induction of DNA lesions. One possible explanation is that in plants, fewer DNA lesions are formed in response to IR, resulting in a lesser insult to the genome. Alternatively, but not exclusively, it is possible that plants possess a greater capacity for DNA repair and/or damage tolerance than do mammals. Thus far it has been difficult to address these questions in plants due to the lack of a method for measuring DSB induction and repair that is both uncomplicated and robust. In this study we describe the development of such a technique and use it to demonstrate that comparable doses of IR appear to induce fewer DSBs in *Arabidopsis* than in mammalian cells. Additionally, using mutants defective in the plant homologues of *ATM* and *ATR*, we demonstrate the contribution of each to the phosphorylation of histone H2AX in response to IR. Because we limit our focus to M-phase nuclei, these data demonstrate a role for *ATR* in γ-H2AX induction distinct from its conventional role during S phase.

IR Induces Fewer γ-H2AX Foci in Plants than in Mammals

γ-H2AX formation is rapid in mammals, with the first molecules observed within 20 s of irradiation. γ-H2AX protein levels continue to rise with peak formation between ~10 and 30 min after irradiation (Rogakou *et al.*, 1998). We found that in plants, γ-H2AX formation was observable soon after irradiation, peaking at some point between 20 and 40 min after exposure. As observed in mammals and fungi, the production of γ-H2AX increases with increasing damage to the DNA. In contrast, however, the number of foci generated per Gy per Gbp is significantly lower in *Arabidopsis* than mammals or fungi. We find that ~1.25–2 γ-H2AX foci/Gy-Gbp are induced in M-phase root tip nuclei. In comparison, 6 foci/Gy-Gbp, shown to be equivalent to 6 DSBs/Gy-Gbp, are induced in human cells (Rothkamm and Löbrich, 2003), and 5.4 DSBs/Gy-Gbp are induced in yeast (Prise *et al.*, 1998). This suggests that IR actually induces less damage per base pair in the plant genome or that plants fail to form foci at a majority of IR-induced damage sites.

Studies performed on γ-H2AX induction in mammalian cells have convincingly demonstrated that each focus is approximately equivalent to one DSB (Sedelnikova *et al.*, 2002; Rothkamm and Löbrich, 2003), with focus formation and loss reflecting DSB induction and repair. Supporting the notion that we too are observing focus formation primarily at DSBs, other investigators, directly assaying DSB formation in plant cells via pulse-field gel electrophoresis (PFGE), have found a relatively low rate of induction of breaks/Gy-Gbp. Yokota *et al.* performed PFGE (Rydberg *et al.*, 1994; Lobrich *et al.*, 1995; Whitaker *et al.*, 1995) in tobacco BY-2 cells and Chinese hamster ovary (CHO) cells to directly quantitate and compare IR-dependent DSB induction. They determined DSB induction in tobacco cells was only one-third the rate of CHO cells (2.0 ± 0.1 vs. 6.6 ± 0.2 DSBs/Gy-Gbp; Yokota *et al.*, 2005), and the consistency of their CHO DSB induction data with previously published data suggests their methodology is reliable (Table 3; Cedervall *et al.*, 1995). This suggests that plants are, like yeast and mammals, forming γ-H2AX foci at DSBs and that the lower rate of focus formation observed in plants is simply due to a lower rate of damage induction by IR.

What is the basis for lower IR-dependent DSB induction in plants? One possibility is that endogenous plant materials can prevent strand breakage by physically intercepting DNA-damaging molecules. As obligate photosynthesizers, plants frequently must cope with oxidative stress because the photosynthetic process forms reactive oxygen species (ROS) that can interact with and damage intracellular components including nucleic acids (Noctor and Foyer, 1998). The same ROS are also induced by IR-mediated ionization of water molecules that, if formed within radical diffusion distance of DNA, can create lesions including DSBs (Friedberg, 1985). To cope with photo-oxidative damage, plants possess a large repertoire of antioxidants (reviewed in Larson, 1988), compounds that effectively eliminate ROS produced via photosynthesis as well as those from nonphotochemical sources. Thus, it is possible that the lower γ-H2AX induction we observe in plants is due to the action of antioxidants that scavenge IR-induced ROS before they encounter DNA.

The finding that IR induces fewer DSBs in plants is consistent with their higher relative radioresistance. Because fewer lesions are induced per Gy, it is reasonable that a higher dose is needed to effect damage comparable to that inflicted upon mammalian and yeast cells. But is the elevated radioresistance observed in plants directly equivalent to the decrease in DSB induction? One way this question can be addressed is to compare the number of DSBs required to effect 50% lethality (LD_{50}) in yeast and mammals, or in the case of *Arabidopsis*, to completely arrest growth. The LD_{50} is ~1.5 Gy for diploid human fibroblasts (Cole *et al.*, 1988) and ~400 Gy, or 250-fold higher, for diploid yeast (Resnick, 1969; Resnick and Martin, 1976). However, because the yeast genome is ~250-fold smaller than that of humans, the LD_{50} values correspond to induction of ~54 and 52 DSBs respectively making them comparable on a per DSB basis. In comparison, 400 Gy is required simply to arrest growth in

wild-type *Arabidopsis* plants (J. Friesner, unpublished results; Hefner *et al.,* 2003), yet the plant's genome is only 25-fold smaller than the human genome. Therefore, even after accounting for the lower rate of DSB induction, it requires between 125 and 200 DSBs to completely arrest growth in *Arabidopsis.*

Arabidopsis ATM *and* ATR *Both Contribute to γ-H2AX Focus Formation*

In addition to *ATM* and *ATR*, a related mammalian protein, the DNA-dependent protein kinase (*DNA-PK*), has been implicated in the γ-H2AX induction response to DSBs (Park *et al.,* 2003; Stiff *et al.,* 2004). Although it is clear that ATM, ATR, and DNA-PK are important for responding to DNA damage and effecting DSBR and/or cell cycle regulation, there are a number of contradictory reports in the current literature about the involvement of each in DSB-dependent γ-H2AX induction. In an early report, a 95% reduction in γ-H2AX focus formation was observed in *atm*-deficient mouse fibroblasts, suggesting that *ATM* was primarily responsible for IR-induced focus formation. On the other hand, more recent studies report normal (Kuhne *et al.,* 2004; Stiff *et al.,* 2004), or at most, only mild reduction (Karlsson and Stenerlow, 2004) in focus formation in primary fibroblasts derived from *atm* patients, making it unclear to what extent *ATM* is involved in IR-dependent γ-H2AX induction. Complicating matters further, in studies that examined γ-H2AX formation in the *DNA-PK*-deficient cell line M059J, one reported atypical focus induction (Paull *et al.,* 2000), whereas two concluded induction was normal (Karlsson and Stenerlow, 2004; Stiff *et al.,* 2004). The difficulty in interpreting these data are compounded by the fact that M059J cells are also partially defective in *ATM* (Chan *et al.,* 1998; Gately *et al.,* 1998).

In contrast to *ATM* and *DNA-PK*, *ATR* is believed to primarily respond to DNA damage that results from replication blockage (Abraham, 2001; Furuta *et al.,* 2003; Ward *et al.,* 2004), although there is evidence that *ATR* can compensate for the absence of *ATM* in certain situations (Siliciano *et al.,* 1997; Cliby *et al.,* 1998). Interestingly, chromosomes in ATR-deficient mouse blastocyst mitotic spreads are extensively fragmented (Brown and Baltimore, 2000), and "fragile sites," regions in the genome that are especially susceptible to genomic instability after replication stress and appear cytologically as gaps or breaks on metaphase chromosomes, are increased 10–20-fold in ATR-deficient cells (Casper *et al.,* 2002). Although these data may suggest that ATR protects against DSB formation via a role in M phase, it appears more likely that these aberrations are actually due to errors that occurred in the preceding S phase and simply become apparent in M phase (Brown and Baltimore, 2000; Casper *et al.,* 2002; Cimprich, 2003). Thus, the combined literature places the functions of *ATR* primarily in situations of replicational distress.

The mammalian studies that seek to determine the relative contribution(s) of PIKK family members to H2AX phosphorylation are hampered by the inability to delete *ATR*, an essential gene in mammals, thus precluding combining *ATR* null alleles with *ATM*, and/or *DNA-PK* deficiencies. Homologues of DNA-PK have not been found in any nonvertebrates, suggesting that *AtATM* and/or *AtATR* are responsible for phosphorylating H2AX in *Arabidopsis*. The lack of *DNA-PK*, and the availability of viable *ATM* and *ATR Arabidopsis* null mutants allowed us to definitively determine the kinases involved in, and their relative contributions to, IR-induced γ-H2AX formation in M-phase cells.

We find that γ-H2AX focus formation in *atm* M-phase nuclei is reduced to <10% the level in wild-type nuclei, suggesting that *AtATM* is primarily responsible for IR-induced γ-H2AX formation in M-phase cells (Table 2). We also find that *atr* single mutants have slightly, but significantly, reduced focus formation in irradiated M-phase cells, suggesting that *ATR* is responsible for a subset of foci independent of those induced by *ATM* (Figure 8, Table 2). Combining *ATM* and *ATR* deficiencies results in complete abolishment of γ-H2AX induction, in M-phase nuclei and cycling cells, demonstrating that these two proteins are complementary, and completely responsible for IR-dependent γ-H2AX induction, at least over the time course we examined (Figure 9, Table 2). Because we restrict our analysis to cells that have already undergone nuclear breakdown, it is clear that the foci we are seeing were induced in M phase. Thus, *ATR* clearly plays a role in damage recognition outside of (as well as within) the context of normal replicative DNA synthesis.

What is the lesion that *ATR* is recognizing? One possibility is that a subset of IR-induced lesions, or their repair intermediates, are characterized by the presence of extensive ssDNA, which, when complexed with replication protein A (RPA), is an attractive substrate for ATR/ATRIP complex binding (Zou and Elledge, 2003). Alternatively, it was recently shown that ATR is necessary for the S-phase DNA cross-link checkpoint in human cells, demonstrating that this lesion, in S-phase cells at least, is recognized preferentially by ATR, and not ATM (Pichierri and Roselli, 2004). Although repair of interstrand cross-links (ICLs) is poorly understood, they are believed to be minor products of IR-induced DNA damage (Friedberg *et al.,* 1995). However, current research suggests that cells must first enter S phase to convert ICLs into DSBs (Niedernhofer *et al.,* 2004; Rothfuss and Grompe, 2004), thus, it remains to be determined what lesion(s) are recognized by *AtATR* in M-phase cells.

In this article, using immunological detection of plant γ-H2AX, we demonstrate that phosphorylation of H2AX occurs rapidly after IR, as in fungi and mammals, and that the rate of γ-H2AX focus formation in plants is about threefold lower, on a per Gy, per Gbp basis, than in mammalian and yeast cells. We also examined γ-H2AX focus formation in *atm* and *atr* plants and determined that *AtATM* is responsible for the majority (~90%) of IR-induced foci in M-phase cells. Focus formation is completely abolished in *atm,atr* double mutants, confirming that *AtATR* is responsible for the residual foci induced in *atm* plants. Significantly, because we limit our examination to M-phase cells, we show that *ATR* contributes to IR-dependent γ-H2AX focus formation in non–S-phase cells, suggesting a novel role for *ATR* in response to IR distinct from its role during replication.

The development of the plant-specific γ-H2AX antibody should be useful for future studies of plant DNA metabolism. Using the γ-H2AX antibody, we have also observed the presence of γ-H2AX in unirradiated floral bud tissue, and in irradiated interphase *atm*-deficient cells (J. Friesner, unpublished observations), suggesting that the conservation of γ-H2AX function will extend to cells undergoing meiotic recombination, as well DNA replication.

ACKNOWLEDGMENTS

Dr. Bo Liu provided expertise, reagents, and equipment required for cytological studies. Dr. Kevin Culligan provided the *atr* and *atr,atm* segregating lines. We are extremely grateful to Dr. Steve Jacobsen and members of his lab for sharing histone preparation protocols and technical advice and to Dr. Y. Yokota for sharing *in press* data (Yokota *et al.,* 2005). We thank Dr. Eli Hefner for ordering the γ-H2AX peptide and antibody. We also thank Drs. Scott

Merlino, Julin Maloof, Dan Kliebenstein, and Steve Theg for helpful discussion; Dr. Julie Lee for technical advice regarding sample preparation and microscopy; and Christy Caldwell and Dr. Ken Kaplan for providing human cells and assistance with immunoblotting. This work was made possible by an National Institute of Environmental Health Sciences fellowship provided to J. Friesner (grant 5-32-ES07059). Support was also provided by United States–Israel Binational Agricultural Research Fund (US-3223-01C) and the United States Department of Agriculture (04-35301-14740).

REFERENCES

Abraham, R. (2001). Cell cycle checkpoint signaling through the ATM and ATR kinases. Genes Dev. *15*, 2177–2196.

Arabidopsis Genome, I. (2000). Analysis of the genome sequence of the flowering plant *Arabidopsis thaliana.* Nature *408*, 796–815.

Barlow, C., Liyanage, M., Moens, P. B., Tarsounas, M., Nagashima, K., Brown, K., Rottinghaus, S., S.P., J., Tagle, D., Ried, T., and Wynshaw-Boris, A. (1998). Atm deficiency results in severe meiotic disruption as early as leptonema of prophase I. Development *125*, 40007–40017.

Brown, E., and Baltimore, D. (2003). Essential and dispensable roles of ATR in cell cycle arrest and genome maintenance. Genes Dev. *17*, 615–628.

Brown, E.J., and Baltimore, D. (2000). ATR disruption lead to chromosome fragmentation and early embryonic lethality. Genes Dev. *15*, 397–402.

Burma, S., Chen, B. P., Murphy, M., Kurimasa, A., and Chen, D. J. (2001). ATM phosphorylates histone H2AX in response to DNA double-strand breaks. J. Biol. Chem. *276*, 42462–42467.

Casper, A. M., Nghiem, P., Arlt, M. F., and Glover, T. W. (2002). ATR regulates fragile site stability. Cell *111*, 779–789.

Cedervall, B., Wong, R., Albright, N., Dynlacht, J., Lambin, P., and Dewey, W. C. (1995). Methods for the quantification of DNA double-strand breaks determined from the distribution of DNA fragment sizes measured by pulsed-field gel electrophoresis. Rad. Res. *143*, 8–16.

Chan, D. W., Gately, D. P., Urban, S., Galloway, A. M., Lees-Miller, S. P., Yen, T., and Allalunis-Turner, J. (1998). Lack of correlation between ATM protein expression and tumour cell radiosensitivity. Int. J. Rad. Biol. *74*, 217–224.

Chen, G. *et al.* (1999). Radiation-induced assembly of Rad51 and Rad52 recombination complex requires ATM and c-Abl. J. Biol. Chem. *274*, 12748–12752.

Chen, H. T. *et al.* (2000). Response to RAG-mediated V(D)J cleavage by NBS1 and gamma-H2AX. Science *290*, 1962–1964.

Cimprich, K. A. (2003). Fragile sites: breaking up over a slowdown. Curr. Biol. *13*, R231–R233.

Cliby, W., Roberts, C., Cimprich, K., Stringer, C., Lamb, J., Schreiber, S., and Friend, S. (1998). Overexpression of a kinase-inactive ATR protein causes sensitivity to DNA-damaging agents and defects in cell cycle checkpoints. EMBO J. *17*, 159–169.

Cole, J., Arlett, C. F., Green, M. H., Harcourt, S. A., Priestley, A., Henderson, L., Cole, H., James, S. E., and Richmond, F. (1988). Comparative human cellular radiosensitivity: II. The survival following gamma-irradiation of unstimulated (G0) T-lymphocytes, T-lymphocyte lines, lymphoblastoid cell lines and fibroblasts from normal donors, afrom ataxia-telangiectasia patients and from ataxia-telangiectasia heterozygotes. Int. J. Radiat. Biol. *54*, 929–943.

Culligan, K. M., Tissier, A., and Britt, A. B. (2004). ATR regulates a G2-phase cell-cycle checkpoint in *Arabidopsis thaliana.* Plant Cell *16*, 1091–1104.

D'Amato, F. (1964). Endopolyploidy as a factor in plant tissue development. Caryologia *17*, 41–52.

Dart, D., Adams, K., Akerman, I., and Lakin, N. (2004). Recruitment of the cell-cycle checkpoint kinase ATR to chromatin during S-phase. J. Biol. Chem. *279*, 16433–16440.

de Klein, A., Muijtjens, M., van, O., s.R., Verhoeven, Y., Smit, B., Carr, A., Lehmann, A., and Hoeijmakers, J. (2000). Targeted disruption of the cell-cycle checkpoint gene ATR leads to early embryonic lethality in mice. Curr. Biol. *20*, 188–189.

Fernandez-Capetillo, O. *et al.* (2002). DNA damage-induced G2-M checkpoint activation by histone H2AX and 53BP1. Nat. Cell Biol. *4*, 993–997.

Friedberg, E. C. (1985). DNA repair. San Francisco: W. H. Freeman and Co.

Friedberg, E. C., Walker, G. C., and Siede, W. (1995). DNA repair and mutagenesis. Washington, DC: ASM Press.

Friesner, J. D., and Britt, A. B. (2003). Ku80- and DNA ligase IV-deficient plants are sensitive to ionizing radiation and defective in T-DNA integration. Plant J. *34*, 427–440.

Furuta, T. *et al.* (2003). Phosphorylation of histone H2AX and activation of Mre11, Rad50, and Nbs1 in response to replication-dependent DNA double-strand breaks induced by mammalian DNA topoisomerase I cleavage complexes. J. Biol. Chem. *278*, 20303–20312.

Garcia, V., Bruchet, H., Camescasse, D., Granier, F., Bouchez, D. L., and Tissier, A. (2003). AtATM is essential for meiosis and the somatic response to DNA damage in plants. Plant Cell *15*, 119–132.

Gatei, M., Young, D., Cerosaletti, K. M., Desai-Mehta, A., Spring, K., Kozlov, S., Lavin, M. F., Gatti, R. A., Concannon, P., and Khanna, K. (2000). ATM-dependent phosphorylation of nibrin in response to radiation exposure. Nat. Gen. *25*, 115–119.

Gately, D. P., Hittle, J. C., Chan, G.K.T., and Yen, T. J. (1998). Characterization of ATM expression, localization, and associated DNA-dependent protein kinase activity. Mol. Biol. Cell *9*, 2361–2374.

Glasunov, A. V., Glaser, V. M., and Kapultsevich, Y. G. (1989). Two pathways of DNA double-strand break repair in G1 cells of *Saccharomyces cerevisiae.* Yeast *5*, 131–140.

Green, R. A., and Kaplan, K. B. (2003). Chromosome instability in colorectal tumor cells is associated with defects in microtubule plus-end attachments caused by a dominant mutation in APC. J. Cell Biol. *163*, 949–961.

Hefner, E. A., Preuss, S. B., and Britt, A. B. (2003). *Arabidopsis* mutants sensitive to gamma radiation include the homolog of the human repair gene *ERCC1.* J. Exp. Bot. *54*, 669–680.

Hush, J., Wu, L., John, P.C.L., Hepler, L. H., and Hepler, P. K. (1996). Plant mitosis promoting factor disassembles the microtubule preprophase band and accelerates prophase progression in *Tradescantia.* Cell Biol. Int. *20*, 275–287.

Iliakis, G., Wang, H., Perrault, A. R., Boecker, W., Rosidi, B., Windhofer, F., Wu, W., Guan, J., Terzoudi, G., and Pantelias, G. (2004). Mechanisms of DNA double strand break repair and chromosome aberration formation. Cytogenet. Genome Res. *104*, 14–20.

Jackson, J. P., Johnson, L., Jasencakova, Z., Zhang, X., PerezBurgos, L., Singh, P. B., Cheng, X., Schubert, I., Jenuwein, T., and Jacobsen, S. E. (2004). Dimethylation of histone H3 lysine 9 is a critical mark for DNA methylation and gene silencing in *Arabidopsis thaliana.* Chromosoma *112*, 308–315.

Karlsson, K., and Stenerlow, B. (2004). Focus formation of DNA repair proteins in normal and repair-deficient cells irradiated with high-LET ions. Rad. Res. *161*, 517–527.

Kodym, R., and Horth, E. (1995). Determination of radiation-induced DNA strand breaks in individual cells by non-radioactive labelling of 3′ OH ends. Int. J. Rad. Biol. *68*, 133–139.

Kuhne, M., Riball, E., Rief, N., Rothkamm, K., Jeggo, P. A., and Lobrich, M. (2004). A double-strand break defect in ATM-deficient cells contributes to radiosensitivity. Cancer Res. *64*, 500–508.

Larson, R. A. (1988). The antioxidants of higher plants. Phytochemistry *27*, 969–978.

Limoli, C. L., Giedzinski, E., Bonner, W. M., and Cleaver, J. E. (2002). UV-induced replication arrest in the xeroderma pigmentosum variant leads to DNA double-strand breaks, gamma-H2AX formation, and Mre11 relocalization. Proc. Natl. Acad. Sci. USA *99*, 233–238.

Liu, B., Joshi, H., and Palevitz, B. (1993). A gamma tubulin related protein associated with the microtubule arrays o higher plants in a cell cycle dependent manner. J. Cell Sci. *104*, 1217–1228.

Lobrich, M., Rydberg, B., and Cooper, P. K. (1995). Repair of x-ray-induced DNA double-strand breaks in specific Not I restriction fragments in human fibroblasts: joining of correct and incorrect ends. Proc. Natl. Acad. Sci. USA *92*, 12050–12054.

Mahadevaiah, S. K., Turner, J.M.A., Baudat, F., Rogakou, E. P., de Boer, P., Blanco-Rodriguez, J., Jasin, M., Keeney, S., Bonner, W. M., and Burgoyne, P. S. (2001). Recombinational DNA double-strand breaks in mice precede synapsis. Nat. Gen. *27*, 271–276.

Mitchell-Olds, T., and Clauss, M. J. (2002). Plant evolutionary genomics. Curr. Opin. Plant Biol. *5*, 74–79.

Nazarov, I. B. *et al.* (2003). Dephosphorylation of histone gamma-H2AX during repair of DNA double-strand breaks in mammalian cells and its inhibition by calyculin A. Rad. Res. *160*, 309–317.

Niedernhofer, L. J., Odijk, H., Budzowska, M., van Drunen, E., Maas, A., Theil, A. F., de Wit, J., Jaspers, N.G.J., Beverloo, H. B., Hoeijmakers, J.H.J., and Kanaar, R. (2004). The structure-specific endonuclease Ercc1-Xpf is required to resolve DNA interstrand cross-link-induced double-strand breaks. Mol. Cell. Biol. *24*, 5776–5787.

Noctor, G., and Foyer, C. H. (1998). Ascorbate and glutathione: keeping active oxygen under control. Annu. Rev. Plant Physiol. Mol. Biol. *49*, 249–279.

Park, E.-J., Chan, D. W., Park, J.-H., Oettinger, M. A., and Kwon, J. (2003). DNA-PK is activated by nucleosomes and phosphorylates H2AX within the nucleosomes in an acetylation-dependent manner. Nucleic Acids Res. *31*, 6819–6827.

Paull, T. T., Rogakou, E. P., Yamazaki, V., Kirchgessner, C. U., Gellert, M., and Bonner, W. M. (2000). A critical role for histone H2AX in recruitment of repair factors to nuclear foci after DNA damage. Curr. Biol. *10*, 886–895.

Pichierri, P., and Roselli, F. (2004). The DNA crosslink-induced S-phase checkpoint depends on ATR-CHK1 and ATR-NBS1-FANCD2 pathways. EMBO J. *23*, 1178–1187.

Prise, K.M. *et al.* (1998). A review of dsb induction data for varying quality radiations. Int. J. Rad. Biol. *74*, 173–184.

Redon, C., Pilch, D., Rogakou, E., Sedelnikova, O., Newrock, K., and Bonner, W. (2002). Histone H2A variants H2AX and H2AZ. Curr. Opin. Gen. Dev. *12*, 162–169.

Resnick, M. A. (1969). Genetic control of radiation sensitivity in *Saccharomyces cerevisiae*. Genetics *62*, 519–531.

Resnick, M. A., and Martin, P. (1976). The repair of double-strand breaks in the nuclear DNA of *Saccharomyces cerevisiae* and its genetic control. Mol. Gen. Genet. *143*, 119–129.

Rogakou, E., Pich, D., Orr, A., Ivanova, V., and Bonner, W. (1998). DNA double stranded breaks induce histone H2AX phosphorylation on serine 139. J. Biol. Chem. *273*, 5858–5868.

Rogakou, E. P., Boon, C., Redon, C., and Bonner, W. M. (1999). Megabase chromatin domains involved in DNA double-strand breaks in vivo. J. Cell Biol. *146*, 905–915.

Rothfuss, A., and Grompe, M. (2004). Repair kinetics of genomic interstrand DNA cross-links: Evidence for DNA double-strand break-dependent activation of the Fanconi anemia/BRCA pathway. Mol. Cell. Biol. *24*, 123–134.

Rothkamm, K., and Löbrich, M. (2003). Evidence for a lack of DNA double-strand break repair in human cells exposed to very low x-ray doses. Proc. Natl. Acad. Sci. USA *100*, 5057–5062.

Rydberg, B., Lobrich, M., and Cooper, P. K. (1994). DNA double-strand breaks induced by high-energy neon and iron ions in human fibroblasts. I. Pulsed-field gel electrophoresis method. Rad. Res. *139*, 133–141.

Sancar, A., Lindsey-Boltz, L. A., Unsal-Kaccmaz, K., and Linn, S. (2004). Molecular mechanisms of mammalian DNA repair and the DNA damage checkpoints. Annu. Rev. Biochem. *73*, 39–85.

Sedelnikova, O. A., Rogakou, E. P., Panyutin, I. G., and Bonner, W. M. (2002). Quantitative detection of (125)IdU-induced DNA double-strand breaks with gamma-H2AX antibody. Rad. Res. *158*, 486–492.

Shiloh, Y. (2003). ATM and related protein kinases: safeguarding genome integrity. Nat. Rev. Cancer *3*, 155–168.

Siliciano, J. D., Canman, C. E., Taya, Y., Sakaguchi, K., Appella, E., and Kastan, M. B. (1997). DNA damage induces phosphorylation of the amino terminus of p53. Genes Dev. *11*, 3471–3481.

Stiff, T., O'Driscoll, M., Rief, N., Iwabuchi, K., Lobrich, M., and Jeggo, P. A. (2004). ATM and DNA-PK function redundantly to phosphorylate H2AX after exposure to ionizing radiation. Cancer Res. *64*, 2390–2396.

van den Bosch, M., Bree, R., and Lowndes, N. F. (2003). The MRN complex: coordinating and mediating the response to broken chromosomes. EMBO Rep. *4*, 844–849.

Vos, J. W., Safadi, F., Reddy, A.S.N., and Hepler, P. K. (2000). The kinesin-like calmodulin binding protein is differentially involved in cell division. Plant Cell *12*, 979–990.

Ward, I., Minn, K., and Chen, J. (2004). UV-induced ATR activation requires replicational stress. J. Biol. Chem. *279*, 9677–9680.

Ward, I. M., and Chen, J. (2001). Histone H2AX is phosphorylated in an ATR-dependent manner in response to replicational stress. J. Biol. Chem. *276*, 47759–47762.

Whitaker, S. J., Ung, Y. C., and McMillan, T. J. (1995). DNA double-strand break induction and rejoining as determinants of human tumour cell radiosensitivity: A pulsed-field gel electrophoresis study. Int. J. Rad. Biol. *67*, 7–18.

Wolniak, S. M., and Larsen, P. M. (1992). Changes in the metaphase transit times and the pattern of sister chromatid separation in stamen hair cells of tradescantia after treatment with protein phosphatase inhibitors. J. Cell Sci. *102*, 691–715.

Yokota, Y., Shikazono, N., Tanaka, A., Hase, Y., Funayama, S., Wada, S., and Inoue, M. (2005).Comparative radiation tolerance based on the induction of DNA double-strand breaks in tobacco BY-2 cells and CHO-K1 cells irradiated with gamma-rays. Rad. Res. (*in press*).

Zou, L., and Elledge, S. J. (2003). Sensing DNA damage through ATRIP recognition of RPA-ssDNA complexes. Science *300*, 1542–1548.